Transition to turbulence in Hunt's flow in a moderate magnetic field

Braiden, LA, Krasnov, D, Molokov, S, Boeck, T & Buhler, L

Original citation & hyperlink:
Braiden, LA, Krasnov, D, Molokov, S, Boeck, T & Buhler, L 2016, 'Transition to turbulence in Hunt's flow in a moderate magnetic field' *EPL*, vol 115, no. 4, 44002
https://dx.doi.org/10.1209/0295-5075/115/44002

DOI 10.1209/0295-5075/115/44002
ISSN 0295-5075
ESSN 1286-4854

Publisher: European Physical Society

Transition to turbulence in Hunt's flow in a moderate magnetic field

L. Braiden[1], D. Krasnov[2], S. Molokov[1], T. Boeck[2] and L. Bühler[3]

[1] *School of Computing, Electronics and Mathematics, Coventry University, Priory Street, Coventry CV1 5FB, UK*
[2] *Institute of Thermodynamics and Fluid Mechanics, Technische Universität Ilmenau, 98684 Ilmenau, Germany*
[3] *Institut für Kern- und Energietechnik, Karlsruher Institut für Technologie, 76021 Karlsruhe, Germany*

PACS 47.35.Tv – Magnetohydrodynamics in fluids
PACS 47.27.Cn – Transition to turbulence
PACS 47.27.N- – Turbulent flows, wall-bounded

Abstract – Pressure-driven magnetohydrodynamic duct flow in a transverse uniform magnetic field is studied by direct numerical simulation. The electric boundary conditions correspond to Hunt's flow with perfectly insulating walls parallel to the magnetic field (side walls) and perfectly conducting walls perpendicular to the magnetic field (Hartmann walls). The velocity distribution exhibits strong jets at the side walls, which are susceptible to instability even at low Reynolds numbers Re. We explore the onset of time-dependent flow and transition to states with evolved turbulence for a moderate Hartmann number $Ha = 100$. At low Re time-dependence appears in the form of elongated Ting-Walker vortices at the side walls of the duct, which, upon increasing Re, develop into more complex structures with higher energy and then the side-wall jets partially detach from the walls. At high values of Re jet detachments disappear and the flow consists of two turbulent jets and nearly laminar core. It is also demonstrated that, there is a range of Re, where Hunt's flow exhibits a pronounced hysteresis behavior, so that different unsteady states can be observed for the same flow parameters. In this range multiple states may develop and co-exist, depending on the initial conditions.

Introduction. – Magnetohydrodynamic (MHD) flows in ducts play a major role in liquid metal blankets for thermonuclear fusion reactors serving for cooling of the reactor and for breeding tritium [1]. A very important requirement to these flows is that they should provide sufficient mixing of the fluid to improve heat and mass transfer characteristics, i.e. provide sufficient level of turbulence. This, however, may be problematic as the liquid metal flow occurs in a high magnetic field of about $5-10$ Tesla. This leads to high MHD interaction between the induced currents $\boldsymbol{j}$ and the magnetic field $\boldsymbol{B}$ resulting in a strong braking Lorentz body force $\boldsymbol{j} \times \boldsymbol{B}$, which tends to damp turbulence.

More often than not the ducts have thin electrically conducting walls, which leads to a velocity profile, shown in Fig. 1. Here the basic velocity exhibits a flat core, exponential Hartmann layers at the walls transverse to the magnetic field (the Hartmann walls), and jets at the walls parallel to the field (the side walls). Jets appear due to induced electric current within the core of the flow. The current must turn (either fully or partially) in the direction of the magnetic field at the side walls to complete the loops, which then close through the conducting Hartmann walls (Fig. 1). Once this happens, the resulting force $\boldsymbol{j}\times\boldsymbol{B}$ and its braking effect are reduced in the near-wall region, thus allowing the fluid to flow with higher velocity than in the core. The exact ratio of the core to jet velocities and thus between the mass fluxes strongly depends on the electrical conductivities of the Hartmann- and side-walls. In the extreme case of perfectly electrically insulating side walls and perfectly conducting Hartmann walls (known as Hunt's flow, see a particular case in [2]), practically all the mass flux is carried by the side-wall jets.

We will be concerned here with an electrically conducting, incompressible fluid flow in a square duct, driven by a mean pressure gradient, with kinematic viscosity, ν, density, ρ, and electrical conductivity, σ. The flow is subjected to a uniform magnetic field of intensity B applied in the z-direction (x, y, z are Cartesian coordinates, as shown in Fig. 1). For a given mean velocity U,

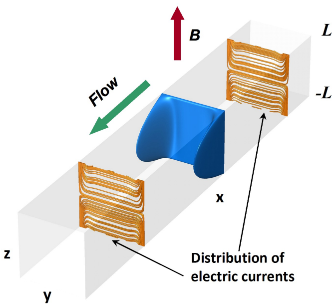

Fig. 1: Flow geometry of Hunt's flow in a square duct. Laminar velocity distribution with perfectly conducting Hartmann- and perfectly insulating parallel-walls is shown at $Ha = 100$ (blue); also shown are the streamlines of electric current density (brown).

the flow is characterised by three dimensionless parameters [3]: the Reynolds number, $Re = UL/\nu$, where L is half the distance between the walls, the Hartmann number $Ha = BL(\sigma/\rho\nu)^{1/2}$, the square of which characterises the ratio between the Lorentz and viscous forces, and the wall conductance ratio $c = \sigma_w h_w/\sigma L$, where σ_w and h_w are the electrical conductivity and thickness of the wall, respectively. Note that c may be different for each wall.

A family of the exact solutions for MHD flows with jets was obtained in [2]. Early experimental results were reviewed in [4], and the main conclusion was that the jets were much thicker than the $O(Ha^{-1/2})$ thickness of the jets in the fully developed flow. Linear stability of a flow in a duct with $c = 0.07$ [5] could not account for this increase in the thickness as the instability was fully contained in the parallel side layers. In addition, the Ting and Walker (TW) vortices appeared for critical Reynolds number $Re_{cr} \sim 300$, while in the corresponding experiment [6] the instabilities appeared at $Re_{cr} \sim 3000$. For Hunt's flow linear stability analysis was performed by [7], who discovered a rich variety of perturbations for $Ha < 45$, while for higher Ha the most unstable mode consisted of TW vortices. The controvercies between the theory and the experiment were resolved in [8], where for $Ha = 200$ and $c = 0.5$ direct numerical simulation (DNS) of the transition to turbulence were performed. First, it was shown that, when TW vortices appear, they are so weak that they do not affect the mean velocity profile. For $Re > 3500$ a new effect appeared consisting of partial jet detachment from the side walls, which indeed led to thicker jets.

In this letter we will focus on the transition to turbulence in Hunt's flow and present various flow structures obtained during the transition. Detailed analysis of these state will be presented later in a series of journal papers.

Procedure and parameters. – We consider the MHD equations for incompressible fluid in a quasi-static form, which is standard for liquid metals (see, e.g., [3,5,8]). The governing equations are solved with second-order finite differences using our in-house solver [9]. The boundary conditions are periodic in the streamwise x-direction. Time integration is either fully explicit (using the 2^{nd} order Adams-Bashforth/Backward-differencing scheme) or with the implicit treatment of the viscous terms $\frac{1}{Re}\nabla^2 \boldsymbol{v}$. The semi-implicit version is beneficial at low-Re, as it helps to maintain large integration time-steps δt without the loss of numerical stability.

The simulations have been conducted in a domain size of $8\pi \times 2 \times 2$ and numerical resolution varied from 512×128^2 to 1024×256^2 points in, correspondingly, x-, y- and z-directions. The computational grid is clustered in the wall-normal y- and z-directions by applying the coordinate transformation based on the hyperbolic tangent (see, e.g., [9]). Constant time step δt was maintained at 5×10^{-4}...2×10^{-3} (depending on Re). The typical runtime contributed to 5×10^{5}...10^{6} steps (several hundreds of convective units) using 128...1024 cores, depending on the resolution.

A series of DNS has been performed at a fixed Hartmann number $Ha = 100$, representing the case of moderate magnetic fields, and a broad range of Re, covering regimes from $Re = 200$ to 10000. A similar approach with fixed Ha was also used in [8]. In various studies on flow transition the most commonly used scenario is to modulate the initially laminar flow by perturbations. These can be either random noise or a combination of specially constructed modes modulated by random noise (one- or two-step scenario, e.g., [10]). In either case the transient evolution and the actual thresholds are governed by many parameters, such as the amplitude of perturbations, specific spatial shape and distribution, optimal wave-numbers, etc. To avoid this ambiguity, two other scenarios of obtaining time-dependent MHD solutions have been adopted. First, we have used fully developed non-MHD turbulent flows, precomputed for the closest possible Re, as the initial state. Then the magnetic field is switched on and the simulation is continued further. This method has the appeal that fluctuations are created in a natural way. In another procedure the unsteady MHD solution, obtained for a certain Re, is used as the initial state to study evolution to a different target Re, which can be either higher or lower than the initial Re. This method has been most extensively used to study the phenomenon of hysteresis. We have employed both ways of changing Re – with small steps and as a single shot to the target value. The onset of new unsteady solutions or transition between different states have been identified by visual analysis of the flow field and by monitoring the kinetic energy of the transverse velocity components $q_t = u_y^2 + u_z^2$ (see, e.g., [11]). To attain a statisticaly sustained (fully developed) state the simulations have typically run for the time from at least 100 to 1000 convective time-units.

Results. –

Low- and mid-range values of Re. We begin our discussion with the results of simulations at $Re = 500$ shown in Fig. 2a. This flow state was obtained using turbulent non-MHD flow at $Re = 1200$ (the smallest Re where turbulence can still exist) as an initial condition. One interesting observation is that the turbulent energy drops by several orders of magnitude as the magnetic field is switched on. Basically, the magnetic field rapidly destroys turbulence so that the remaining perturbations can be viewed as a residual noise. As a minimum is attained, the residual fluctuations start to grow and finally evolve into a different unsteady regime. This behavior has been found in our simulations performed at other values of Re.

Here we can clearly observe inherently small vortical structures located within the side layer region (Fig. 2a and insert). The vortices exhibit anisotropy in the vertical z-direction, especially pronounced close to the Hartmann walls, as illustrated by the isosurfaces of λ_2-criterion. According to [12], negative regions of λ_2 identify coherent vortical structures (λ_2 is the 2^{nd} eigenvalue of the tensor $S_{ik}S_{kj} + \Omega_{ik}\Omega_{kj}$, where S_{ij} and Ω_{ij} are the rate of strain and vorticity tensors). The structures are comprised of clockwise rotating vortices (CW, thinner ones at the side walls) and counter clockwise rotating vortices (CCW, thicker ones closer to the core). Hereafter the direction of vortex rotations is conventionally defined in respect to the right-side if viewed along the flow direction (note the sign change at the opposite wall). Both CW and CCW vortices are organized in a slightly staggered arrangement. These are the so-called TW vortices [5], they appear at low-Re and are viewed as the 1^{st} unstable solution of Hunt's flow. The TW vortices are very weak, e.g., for this case their kinetic energy is about 0.033% of the total kinetic energy of the flow (Table 1), so hardly producing any visible impact on the integral flow charachteristics, such as the wall stresses τ_w or the total friction coefficient C_f.

Further increase of Re reveals an interesting and rather unexpected behavior of the flow. Namely, using this state as the initial condition and increasing Re to 1000, we have observed that TW vortices very quickly and nearly completely disappear during the initial phase of simulation. However, after about a hundred of convective units of temporal evolution, a new type of vortical structrures is developed. These new instabilities are much larger, both in size and kinetic energy (about 0.1% of the total kinetic energy), are elongated in the flow direction and tend to dominate about 50...60% of the flow domain (Fig. 2b). This particular behavior is observed in the range $1000 \leq Re \leq 1300$, where these big vortical structures have also been repeatedly reproduced in simulations initiated by non-MHD turbulent states.

Increasing Re to 1400, we again observe another flow regime. New structures develop in the form of additional small-scale CW and CCW rotating vortices, which are located within the large instabilities previously observed at $1000 \leq Re \leq 1300$, which evolve in this case too. There are quite a few remarkable features concerning these structures. On the initial inspection, they are very small in size and elongated in the vertical z-direction, as demonstrated in Fig. 2c and in Table 1. The shape resembles that of "pike-teeth", which are settled in a staggered arrangement in respect to the mid-plane symmetry $z = 0$. Further analysis shows that the kinetic energy of these new structures is about two times smaller than the previous instabilities at $Re \leq 1300$, contributing 0.05% of the total kinetic energy of the flow. However, the specific distribution of the kinetic energy over velocity components changes. Albeit the streamwise component is still dominating, the energy associated with the vertical component increases by a factor of 2, thus producing stronger anisotropy in the vertical direction (e.g., q_z/q_y in Table 1). Basically, the "pike-teeth" can be viewed as rather strong (in amplitude) and short (in the vertical length) modes. Once these structures have developed, they remain in the flow throughout the simulation. At higher Re (up to 1550) they develop more rapidly, stretching in the vertical direction, and demonstrate an alternating behavior along the side walls.

To check the validity of the results we have conducted additional verifications. First, it has been found that these structures also arise if the simulation is initiated with turbulent state. Secondly, to make sure these structures were not a numerical artifact due to an insufficient grid, we have also performed simulations at higher resolution of 2048×384^2 points and found them to appear again.

The "pike-teeth" have been observed in a narrow range $1400 \leq Re \leq 1550$, beyond which they are followed by another type of instability – jet detachments, discussed in the next section. Given the narrow range of Re and the gradually increasing level of kinetic energy, it seems feasible that the "pike-teeth" may serve a nuclei of detachments.

Jet detachments and transition to turbulence. Upon further increase of Re to 1630, we observe that the flow exhibits another time-dependent regime – partial jet detachments. The temporal evolution and settlement of this flow regime is shown in Fig. 3 with four phases, corresponding to the different times of flow evolution. One can see that at the beginning a very small nuclei of instability – a localized spot – appears at one side wall of the duct (a). As time evolves, this spot grows in size and attains kinetic energy from the mean flow until the side jet visibly detaches from the wall (b). Soon after, the detached structure interacts with the opposite side layer, thus, producing a series of small disturbances (c), which rapidly evolve into similar-sized patterns. Consequently, both walls become populated with detached structures (Fig. 3d).

The nature of jet detachments can be understood more thoroughly from the analysis of vortex patterns formed at the side walls, as shown in Fig. 4 for $Re = 2000...5000$. The plot at $Re = 2000$ (Fig. 4a) demonstrates small CW rotating vortices, housed at the inner (near wall) region of the domain of the high velocity jet. They are the result of high shearing effects within the inner region of the duct. Simultaneously, CCW vortices are formed between the outer region of the velocity jet and the core flow. Initially, at $Re \leq 1600$, the small CCW vortices remain stable travelling in the streamwise direction along with the bulk of the flow. At some point the CCW vortices develop both in size and intensity and have a retarding effect on the jet velocity in the outer region. Eventually the CCW vortices

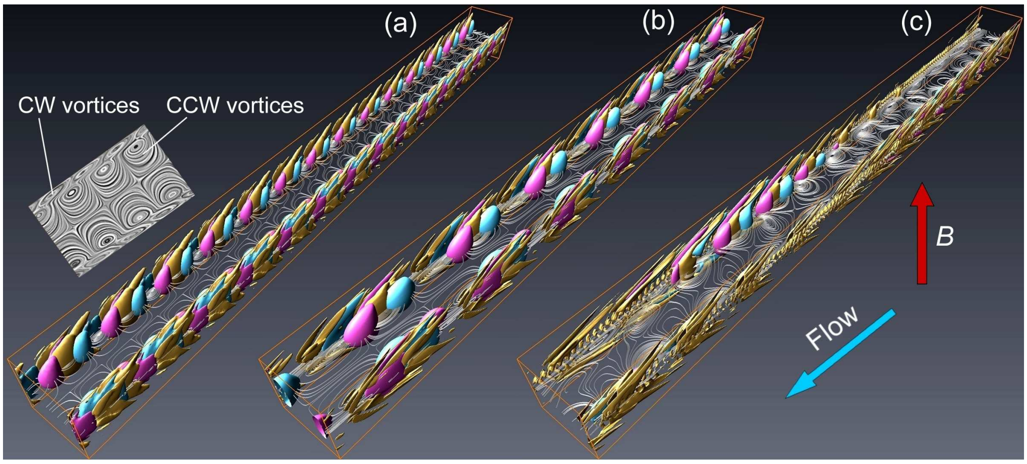

Fig. 2: Instantaneous snapshots of flow states at $Re = 500$ (a), 1000 (b) and 1400 (c). Shown are isosurfaces of the second eigenvalue λ_2 of tensor $S_{ik}S_{kj} + \Omega_{ik}\Omega_{kj}$ (gold) and two isosurfaces of the spanwise velocity component u_y – positive (pink) and negative (cyan) of the same magnitude. The insert shows structure of CW and CCW vortices for $Re = 500$ in the mid-plane $z = 0$ using fluctuating velocity $\boldsymbol{v}$, rotation is defined in respect to the right-side if viewed along the flow direction.

Re	regime	q/Q_{tot}	q_t/Q_{tot}	q_y/q	q_z/q	regime	q/Q_{tot}	q_t/Q_{tot}	q_y/q	q_z/q
	Incremental simulations					Decremental simulations				
300	laminar					jet detach.	2.8%	0.45%	13.7%	2.4%
500	TW vort.	0.033%	0.0081%	11.0%	13.5%	jet detach.	6.3%	1.2%	16.1%	2.9%
1000	large vort.	0.10%	0.0125%	4.0%	8.5%	jet detach.	9.5%	2.1%	18.0%	4.0%
1400	pike-teeth	0.05%	0.0110%	4.0%	18.0%	jet detach.	not performed			
2000	jet detach.	10.0%	2.7%	19.0%	8.0%	jet detach.	same as incremental run			
5000	turb. jets	3.5%	1.5%	17.0%	26.0%	turb. jets	same as incremental run			

Table 1: TKE of velocity perturbations, shown in respect to the total kinetic energy of the flow Q_{tot} and as distribution over different components of the velocity fluctuations. Listed are the TKE of all perturbations $q = \langle u_x^2 + u_y^2 + u_z^2 \rangle$ and the transverse part $q_t = q_y + q_z$, where $q_y = \langle u_y^2 \rangle$ and $q_z = \langle u_z^2 \rangle$. The brackets $\langle\rangle$ stand for volume averaging, u_x is without mean flow, corresponding flow regimes are also indicated.

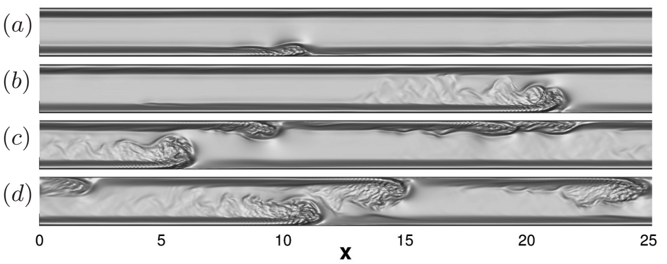

Fig. 3: Temporal evolution of jet detachments at $Re = 1630$ and $Ha = 100$. Full streamwise velocity U_x is shown in the (x, y)-mid-plane at $z = 0$, corresponding to four phases of evolution (every 7 convective units), beginning from a single event on one side-wall to the fully developed unsteady behavior (from top to bottom). Flow direction is from left to right, magnetic field vector is perpendicular to the (x, y)-plane.

have developed sufficiently enough to dramatically alter the flow regime and lift the jet away from the side wall in the y-direction, thus, the first jet detachment occurs. Once a detachment has occurred, its evolution pushes the large CCW vortex through the core flow and hits the opposite layer. Here it interacts with CCW vortices on the opposite wall, thus generating one more detachment. The phenomenon of jet detachments is not entirely new, it has been observed in hydrodynamic flows [13].

Further analysis has been conducted to address the dynamics of jet detachments and to explore the evolution towards even higher Re. We have performed a series of additional simulations and found that a staggered arrangement of partial jet detachments, as in [8], seems to be the preferred pattern. At the same time, the number of structures detached from the side walls is rather ambiguous: not only may it depend of the initial conditions, but also may change during the simulation. In some cases, we have observed non-symmetric flow states with only one wall populated by the spots, whereas the opposite layer remained unaffected for an extended period, sometimes for more than a hundred of convective time units. The evolution at increasing Re (Fig. 4b, c) indicate that the jet detachments gradually lose their characteristic form and develop small-scale structures in their trailing tail. It is clearly evident that already at $Re = 4000$ the side jets have become almost turbulent, albeit rare detachments are still present. Finally, at $Re = 5000$ (Fig. 4d) the side wall regions become entirely turbulent. A remarkable feature is the near stabilization of the core flow as Re increases, which is particularly well observed at $Re \geq 5000$.

Multiple solutions. In the previous sections we have demonstrated various flow regimes and, correspondingly,

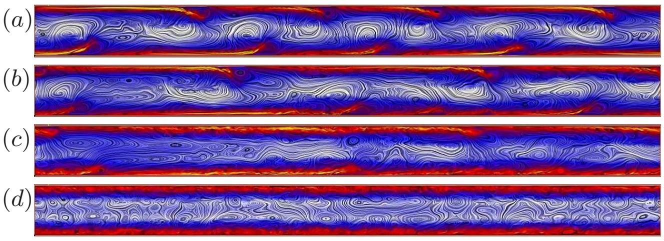

Fig. 4: Transition of states with jet detachmens towards fully tubulent side-wall jets shown for $Re = 2000$ (a), 3000 (b), 4000 (c) and 5000 (d). Instantaneous vortical patterns in the (x, y)-mid-plane are visualized by the streamlines of fluctuating velocity field $\boldsymbol{v}$. Color gradient is highlighted by the magnitude of full-scale streamwise velocity component U_x. Flow direction is from left to right, magnetic field vector is perpendicular to the (x, y)-plane.

the appearance of different types of instabilities, as Re is increased as a single shot or, alternatively, as the magnetic field is instantly switched on. Here we study the flow evolution with yet another approach – changing Re in steps, applying either increments (moving up) or decrements (moving down the Re axis). For the incremental simulations, the initial state at $Re = 500$ and $Ha = 100$, populated with weak TW vortices, have been used. Intrinsically, during the incremental runs we have not found any remarkable differences to the previously obtained results. All flow regimes and the corresponding types of instabilities have been identified at essentially the same ranges of Re, e.g., elongated vortices at $Re = 1000...1100$, "pike teeth" at 1400, beginning of jet detachments at 1600...1700 and turbulization of the side jets at $Re > 4000$.

The situation changes in reverse simulations, starting from a state of $Re = 10000$ with turbulent side jets. The initial and relatively long part between $10000 \geq Re \geq 2000$ demonstrates the reverse sequence of flow regimes vs. the incremental runs, i.e. gradual transition from turbulence to jet detachments (Table 1). However, a continued further decrease of Re reveals no appearance of other intability types, identified in the incremental simulations. Instead, unstable flow regimes with jet detachments continue until $Re \sim 200$, albeit the kinetic energy of perturbations gradually decreases. This behavior demonstrates the phenomenon of multiplicity of possible states and solutions, which appear depending of the particular route. A remarkable feature is that this behavior has been observed in a very broad range $200 < Re < 2000$, inherently in the parameter space varying by one order of magnitude. Similar hysteresis effects were also observed in the prior study of duct flow with finite wall conductivity [8]. However, the range of Re with multiple states was far more narrow. An example of such co-existing solutions is shown in Fig. 5 for two different flow states at the same $Re = 1000$. We can see both the pattern typical for CW and CCW vortices (Fig. 5, top) and jet detachments (Fig. 5, bottom) obtained in, correspondingly, incremental and decremental simulations. Our further investigations have shown that the multiplicity is not only affected by the direction of varying Re, but also by the initial conditions (e.g., uncorrelated turbulent non-MHD states).

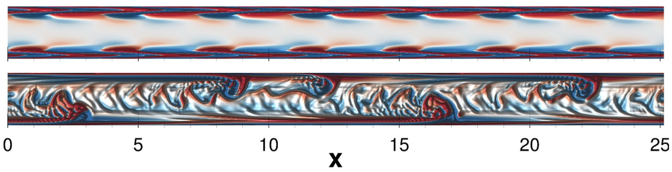

Fig. 5: Instantaneous snapshots of flow fields at $Re = 1000$ shown for incremental (top) and decremental (bottom) simulations. The flow patterns are visualized by the vertical vorticity component ω_z in the (x, y)-mid-plane ("blue–red" gradient corresponds to "negative–positive" ranges of ω_z).

This figure also demonstrates another interesting effect – the phenomenon of vortex shedding in the form similar to that of a Kármán street. We have found that this effect is predominantly expressed at low-Re range. The motion of detached structures through the domain generates a vortex shedding in their downwind, thus, producing patterns similar to flows past a solid obstacle.

Summary. – The instability of Hunt's flow has been studied numerically at a fixed $Ha = 100$, which corresponds to moderate magnetic fields, and a broad range of Re varying from 200 to 10000. Upon increasing Re several unsteady flow regimes have been identified, including the TW vortices (low $Re < 1000$), partial jet detachments (mid-range of $Re \geq 1630$) and transition to fully developed turbulence in the side-wall jets (upper range of $Re \geq 5000$). In addition, two new instabilies are discovered: large elongated vortices ($1000 < Re < 1400$) and very small, tightly localized at the side walls, vertical "pike-teeth" structures ($1400 < Re < 1550$). The results of our simulations suggest that these structures can be viewed as transients, connecting the other, major types of unstable solutions. Indeed, these two new regimes are found in rather narrow ranges of Re, being quickly followed by, or proceeded by another persistent unsteady solution, when Re slightly changes.

Our simulations also suggest another view on the instability of Hunt's flow. Namely, given the extremly low amplitude of TW vortices observed at low-Re, one may speculate that the actual transition to the truly unsteady flow states should be viewed beginning from the appearance of jet detachments. By adopting this point of view, we can see the laminar-turbulent transition in Hunt's flow is not a unique feature, but is rather similar to other MHD and non-MHD shear flows. Indeed, approaching the critical range of $Re \approx 1600$, detachments first appear in the form of sporadic events, i.e. essentially isolated spots residing in the side wall layers. As Re increases, the side layers become increasingly populated with such spots, which keep developing small-scale fluctuations, until the entire extent of the side layer is involved into fully turbulent motion, as demonstrated in Fig. 6. Very similar flow dynamics with puffs bordering laminar and turbulent regimes is well known for many other shear flows, in particular for

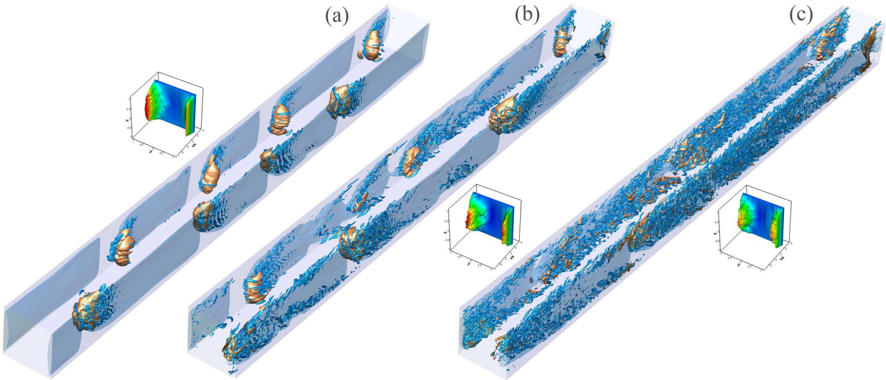

Fig. 6: Evolution of jet detachments versus Re, instantaneous snapshots of flow fields are visualized at $Re = 2000$ (a), 3000 (b) and 4000 (c). Shown are the isosurfaces of full-scale streamwise velocity U_x at the side walls (light blue), TKE of transverse velocity $u_y^2 + u_z^2$ (gold) and λ_2 criterion (cyan). The inserts show velocity profiles in the (y, z)-section at $x = L_x/2$.

MHD duct and pipe flows with insulating walls [11], where the puffs are localized at the side walls. Even the non-symmetry of pattern arrangements at the opposite side walls is observed too. The clearly novel feature of Hunt's flow instability is that these transient states are observed in a much broader range of Re, distinguishing it from other shear flows. The same observation also applies to multiple states and hysteresis, found in an extremely broad range $2000 > Re > 200$.

At the early stages of jet detachments, the vortical structure detaching from the wall can also produce the effect very similar to that of an obstacle, which is observed since the velocity of the core flow is much smaller than in the jet. As a result, the phenomenon of vortex shedding may form.

Another distinct feature we have observed is the non-monotonic behavior of the core flow versus increasing Re number: essentially unperturbed core flow at low-Re regimes (TW vortices), evolution into a strong unsteady motion at moderate Re (jet detachments) and approaching almost unperturbed state, populated with weak quasi-2D structures at high Re (turbulent side-wall jets). This particular behavior of the core flow has practical implications. Namely, the most unsteady regimes at intermediate values of Re seem the most preferred ones to intensify flow mixing and, correspondingly, enhance heat transfer, which is the ultimate purpose of fusion blankets.

* * *

L. Braiden is grateful to the Engineering and Physical Sciences Research Council and Culham Centre for Fusion Energy (UK) for the award of an Industrial CASE PhD studentship. Part of his work was carried out within the framework of the EUROfusion Consortium and has received funding from the Euratom research and training programme 2014-2018 (grant agreement No 633053). D. Krasnov gratefully acknowledges financial support by the Helmholtz-Alliance LIMTECH. Computer resources were provided by the computing centers of Coventry University, Forschungszentrum Jülich (NIC) and TU Ilmenau.

REFERENCES

[1] Bühler. Liquid metal magnetohydrodynamics for fusion blankets. In R. Moreau S. Molokov and H. K. Moffatt, editors, *Magnetohydrodynamics - Historical Evolution and Trends*, pages 171–194. Springer, 2007.

[2] J. C. R. Hunt. Magnetohydrodynamic flow in rectangular ducts. *J. Fluid Mech.*, 21:577–590, 1965.

[3] U. Müller and L. Bühler. *Magnetohydrodynamics in channels and containers*. Springer, Berlin, 2001.

[4] O. Lielausis. Liquid-metal magnetohydrodynamics. *Atomic Energy Review*, 13:527–581, 1975.

[5] A. L. Ting, J. S. Walker, T. J. Moon, C. B. Reed, and B. F. Picologlou. Linear stability analysis for high-velocity boundary layers in liquid-metal magnetohydrodynamic flows. *Int. J. Engng. Sci.*, 29(8):939–948, 1991.

[6] C. B. Reed and B. F. Picologlou. Side wall flow instabilities in liquid metal mhd flow under blanket relevant conditions. *Fusion Techn.*, 15:705–715, 1989.

[7] J. Priede, S. Aleksandrova, and S. Molokov. Linear stability of Hunt's flow. *J. Fluid Mech.*, 649:115–134, 2010.

[8] M. Kinet, B. Knaepen, and S. Molokov. Instabilities and Transition in Magnetohydrodynamic Flows in Ducts with Electrically Conducting Walls. *Phys. Rev. Lett.*, 103:154501, 2009.

[9] D. Krasnov, O. Zikanov, and T. Boeck. Comparative study of finite difference approaches to simulation of magnetohydrodynamic turbulence at low magnetic Reynolds number. *Comp. Fluids*, 50:46–59, 2011.

[10] P. J. Schmid and D. S Henningson. *Stability and Transition in Shear Flows*. Springer, Berlin, 2001.

[11] D. Krasnov, A. Thess, T. Boeck, Y. Zhao, and O. Zikanov. Patterned turbulence in liquid metal flow: Computational reconstruction of the Hartmann experiment. *Phys. Rev. Lett.*, 110:084501, 2013.

[12] J. Jeong and F. Hussein. On the identification of a vortex. *J. Fluid Mech.*, 285(1):69–94, 1995.

[13] R. A. Bajura and M. R. Catalano. Transition in a two-dimensional plane wall jet. *J. Fluid Mech.*, 70:773–799, 1974.